

Research Article

Garlic Peel Surface Modification and Fixed-Bed Column Investigations towards Crystal Violet Dye

E. Pravin Raaj,¹ K. Bhuvaneshwari,¹ R. Lakshmi pathy ,² V. Vandhana Devi,¹
and Ivan Leandro Rodriguez Rico ³

¹Department of Civil Engineering, KCG College of Technology, Karapakkam, Chennai 600097, India

²Department of Chemistry, KCG College of Technology, Karapakkam, Chennai, 600097, India

³Faculty of Chemical and Pharmacy, Department of Chemical Engineering, Central University "Marta Abreu" of Las Villas, Cuba

Correspondence should be addressed to R. Lakshmi pathy; lakshmi pathy.che@kcgcollege.com
and Ivan Leandro Rodriguez Rico; ivanl@uclv.edu.cu

Received 6 July 2022; Revised 31 July 2022; Accepted 9 August 2022; Published 25 August 2022

Academic Editor: Debabrata Barik

Copyright © 2022 E. Pravin Raaj et al. This is an open access article distributed under the Creative Commons Attribution License, which permits unrestricted use, distribution, and reproduction in any medium, provided the original work is properly cited.

Garlic peel, a low-cost agro-waste, was explored as an adsorbent for the remediation of wastewater containing the crystal violet (CV) cationic dye. The garlic peel was treated with NaOH at 1:1.5 ratios in order to modify the surface and increase its porosity. The surface-modified garlic peel was ground to a smaller size in order to increase its surface area and used as an adsorbent in the continuous column investigations. Column parameters such as bed height, flow rate, and initial concentration were optimised and found that optimal removal efficiency was achieved at 3 ml rate of flow, 3 cm column depth, and 100 mg l⁻¹ initial concentration. The surface-modified garlic peel exhibited a higher loading capacity of 99.9 mg g⁻¹ towards CV at optimised conditions. SEM investigations confirmed the surface modification and increase in porosity of the garlic peel. The column data was tending to fit well with Thomas and Yoon-Nelson's models suggesting the scalability to an industrial level. Regeneration of MGP was successful with 0.01 M HCl solution. These results conclude that garlic peel is a potential agro-waste material that can be used to mitigate water pollution.

1. Introduction

Environmental pollution is considered to be one of the biggest threats to human and animal life and number of mortalities reported due to environmental pollution is rising year by year [1]. Industrial revolutions in developed and developing countries are one major source for environmental pollution. Textile and dyeing industries are inevitable part of our life and these industries utilise various dyes for manufacturing and the effluents released from these industries are not fit for use in any forms. Hence, it is highly desirable to treat the effluents from textile and dyeing industries prior to its release or reuse. Treatments techniques include chemical oxidation [2], photodegradation [3], biological process [4], and adsorption [5].

All the treatment techniques have their own merits and demerits; however, adsorption is a powerful and dominant

technique compared to other techniques that are used in treatment process. Various adsorbents such as activated carbon [6], zeolites [7], agro-wastes [8], nanomaterials [9], and composites [10] are successfully demonstrated for the treatments of coloured water especially dye-loaded wastewaters. Agro-wastes find special applications in adsorption due to their cost and eco-friendly nature and their availability. Several agro-wastes have been reported in the literature to date for the remediation of cationic and anionic dyes from wastewater. Untreated agro-wastes suffer from poor adsorption capacity due to low porosity and presence of cations. The adsorption capacity of agro-wastes can be improvised to a greater extent by surface modification and chemical treatments [11]. Inline to the modifications, this study aims at use of a surface-modified agro-waste as an adsorbent for the elimination of synthetic dyes from aqueous solution.

Garlic is a common and key ingredient used in several recipes prepared all over the world and the peel waste is usually discarded due to its unpleasant taste. The garlic peel (GP) waste usually contributes for 16-20% mass of the garlic which amounts to approximately 3 million tons per year [12]. The peels are rich in nutrients and often used in composting and it can be effectively utilised as adsorbents. Hameed and Ahmed proposed garlic peel as an adsorbent for the methylene blue removal from aqueous solution in batch process [13]. Liang et al. suggested the use of garlic peel for the elimination of multi-metal ions from wastewater [14]. Asfaram et al. highlighted the use of garlic peel in removal of direct red 12B as an economical adsorbent [15]. In another study, Liu et al. reported the comparative investigation of native and mercerised garlic peel for the removal of Pb ions [16]. Yanjun et al. chemically modified the garlic peel as used in the adsorption of quinolone antibiotics [17]. In spite of its abundant availability and tendency, the garlic peels are less explored and their ability towards organic contaminants remediation must be established.

This study aims at surface modifications of garlic peels with caustic and further investigates its efficiency towards crystal violet removal in continuous process. The novelty of this investigation is the surface modification of low-cost adsorbent such as garlic peel with economical reagent such as NaOH and employing it in fixed-bed column investigations.

2. Materials and Methods

2.1. Garlic Peel Adsorbent Preparation. Garlic peels (GP) were collected from local agro industry and the peels were washed with tap water to remove any dirt and dust. The water-washed peels were dried under sunlight for four days and later it was ground to small pieces. For surface modifications, garlic peel and sodium hydroxide were mixed in 1 : 1.5 ratios and heated at 100°C for 120 min in a hot air oven. Post heat treatment, the peels were washed with excess water to remove the sodium hydroxide and bring it to neutral pH. The water-washed peel samples were once again dried in oven at 100°C for 120 min and dry samples were kept named as modified garlic peels (MGP) and stored in containers for further use.

2.2. Stock Solution. The stock solution was made by dispersing exactly 1 g of crystal violet dye in 1 L of distilled water. Later, appropriate lower dilutions were made depending on the requirements.

2.3. Fixed-Bed Studies. Fixed-bed studies are considered to be one of the important and prominent investigations in the case of real-time water treatment at industry level. Since the preliminary data obtained can be scaled up to industrial scale level, these studies find unique attention among the community. Investigations were performed for the elimination of crystal violet dye from synthetic solutions with MGP as an adsorbent. The MGP (approximately 0.862 g cm⁻¹) was packed in a pencil column of 20 cm height with an internal diameter of 2 cm. The CV stock was allowed from the top of the column at a fixed rate controlled with a peristaltic

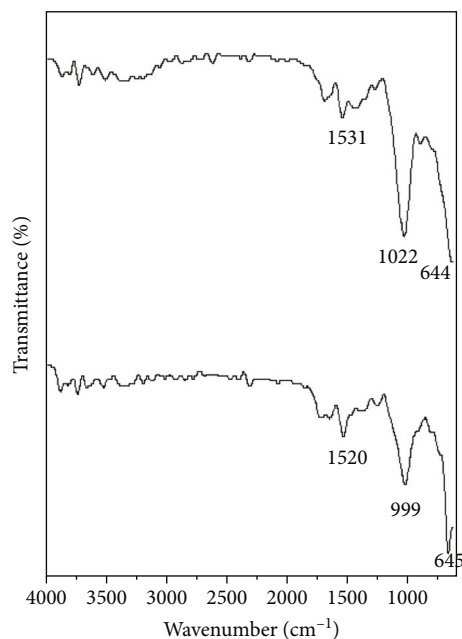


FIGURE 1: FTIR spectra of modified and unmodified garlic peels.

pump. Column parameters such as flow rate, bed height, and initial concentration were tested and optimised. Each parameter under investigation was varied while keeping the other parameters constant. The flow rate was investigated between 3 and 7 ml, bed height at 1, 2, and 3 cm, and initial concentrations between 100 and 300 ppm. The inlet of CV solution was continued until the concentration of input and output remains the same considering the column is saturated [18]. All the samples collected were subjected to UV-visible spectrophotometer to determine the residual concentration of CV at 590 nm.

2.4. Data Analysis. The output of any fixed-bed columns is generally expressed as breakthrough curves and the dynamic behaviour of the columns can be understood by the curve shapes which is considered to be crucial characteristic [19]. The S form curves obtained in breakthrough curves are examined when the output concentration of column reached 0.1% of input concentration and the same is considered to be saturated when the concentration reached 95% of influent. Finally, the volume of effluent (V_{eff}), amount of CV uptake (D_{ad}), absolute quantity of CV dye (D_{total}), and removal % of CV can be determined by the following equations:

$$V_{\text{eff}} = Qt_{\text{total}}, \quad (1)$$

where the volumetric flow rate is denoted with V_{eff} and the total flow time with t_{total} .

$$D_{\text{ad}} = \frac{Q}{1000} \int_{t=0}^{t=t_{\text{total}}} C_{\text{ad}} dt, \quad (2)$$

where C_{ad} is the quantity of CV removed.

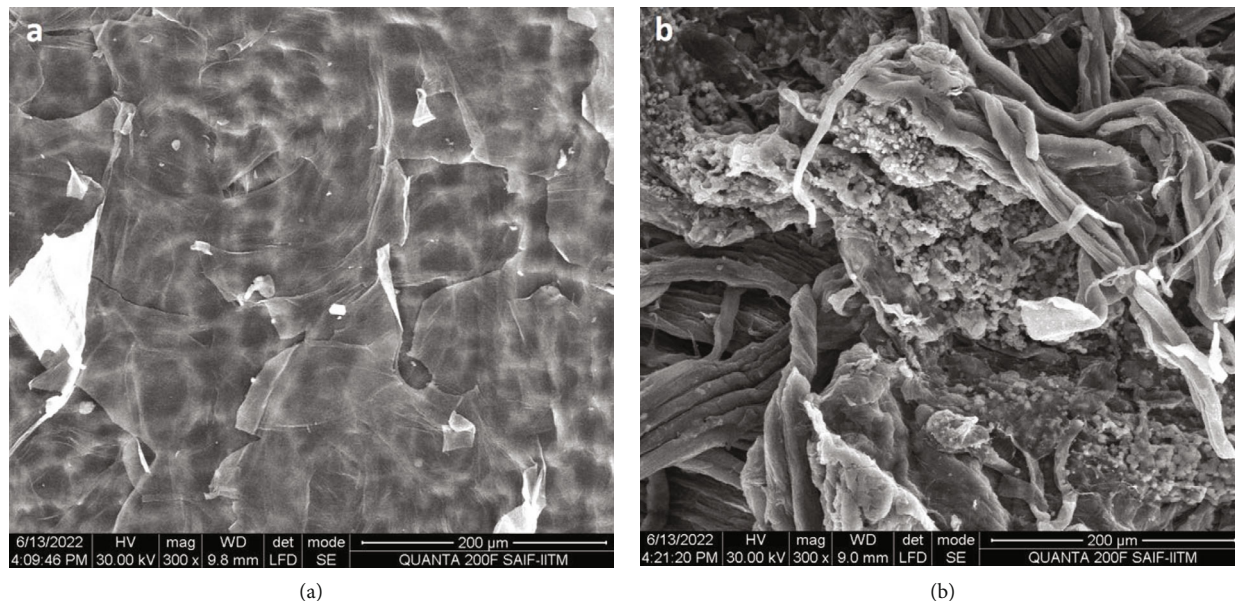


FIGURE 2: SEM image of (a) unmodified GP and (b) modified GP.

$$D_{\text{total}} = \frac{C_0 Q_{\text{total}}}{1000}, \quad (3)$$

$$R(\%) = \frac{D_{\text{ad}}}{D_{\text{total}}} \times 100, \quad (4)$$

where $R(\%)$ is the removal percentage.

2.5. Adsorbent Characterisation. The surface-modified garlic peel was characterised with Fourier Transform Infrared (FTIR), Scanning Electron Microscope (SEM), and Energy Dispersive X-ray (EDX) techniques to understand the changes and modifications. The FTIR analysis was carried out between 4000 and 400 cm^{-1} in Thermo Nicolet Avater 360 equipment. The SEM images of unmodified and modified garlic peels were captured with Quanta 200F FEI instrument equipped with EDX detector. The elemental composition of the garlic peel was obtained from EDX detector of SEM instrument.

3. Results and Discussion

The modified garlic peel (MGP) was subjected to FTIR, SEM, and EDX analyses in order to determine the surface functional groups, porosity, and elemental changes in comparison to the unmodified garlic peel.

The FTIR spectra of modified and unmodified garlic peels are shown in Figure 1. The FTIR spectra displayed were few intense peaks for unmodified garlic peel. A weak peak at 1720 cm^{-1} corresponding to stretching vibrations of carbonyl group (C=O) and a sharp medium peak at 1531 cm^{-1} corresponding to stretching vibrations C-C ring were observed. A strong sharp peak at 1022 corresponds to C-C bending vibrations of esters. A strong sharp peak at 645 corresponds to the metal-oxide bond vibration which is attributed to Ca-O bond since the presence of calcium in

garlic peels is evident from EDX patterns. It is observed that the functional groups and peaks remain unchanged even after surface modification with NaOH suggesting that the surface modification has not impacted the functional groups present on the garlic peels.

The SEM images of unmodified and modified garlic peels are represented in Figure 2. The surface of unmodified garlic peel is smooth with no evidence of porosity (Figure 2(a)). In the case of modified garlic peel, the surface is not smooth as seen in the unmodified garlic peel and the surface looks completely distorted during the treatment with NaOH (Figure 2(b)). The fibres of garlic peel are exposed and look porous in nature. These observations suggest that the surface modification is successfully achieved with NaOH.

The EDX patterns of the modified and unmodified garlic peels are represented in Figure 3. It is noticed that the unmodified garlic peel contains various minerals such as Ca, Mg, K, and Cl (Figure 3(a)). After surface treatment with NaOH, the elements such as Mg and K disappeared and these might have leached out during the treatment process (Figure 3(b)). Na element peak suggests the incorporation of Na ions on the surface during the treatment step. Additional elements observed in the modified GP might be due to surface contaminations.

3.1. Optimization of pH of the Solution. The presence of hydronium ion greatly influences any sorption process and system and it is imperative to optimise the H^+ concentration of the solution before the fixed-bed column studies are embarked. To understand the optimum pH of the solution; investigations were performed in batch process to optimise the H^+ concentration of the solution. The pH was varied between pH2 and 10 by fixing the other variables such as dose, time, and concentration. The results of the investigation are shown in Figure 4 and it can be noticed that with

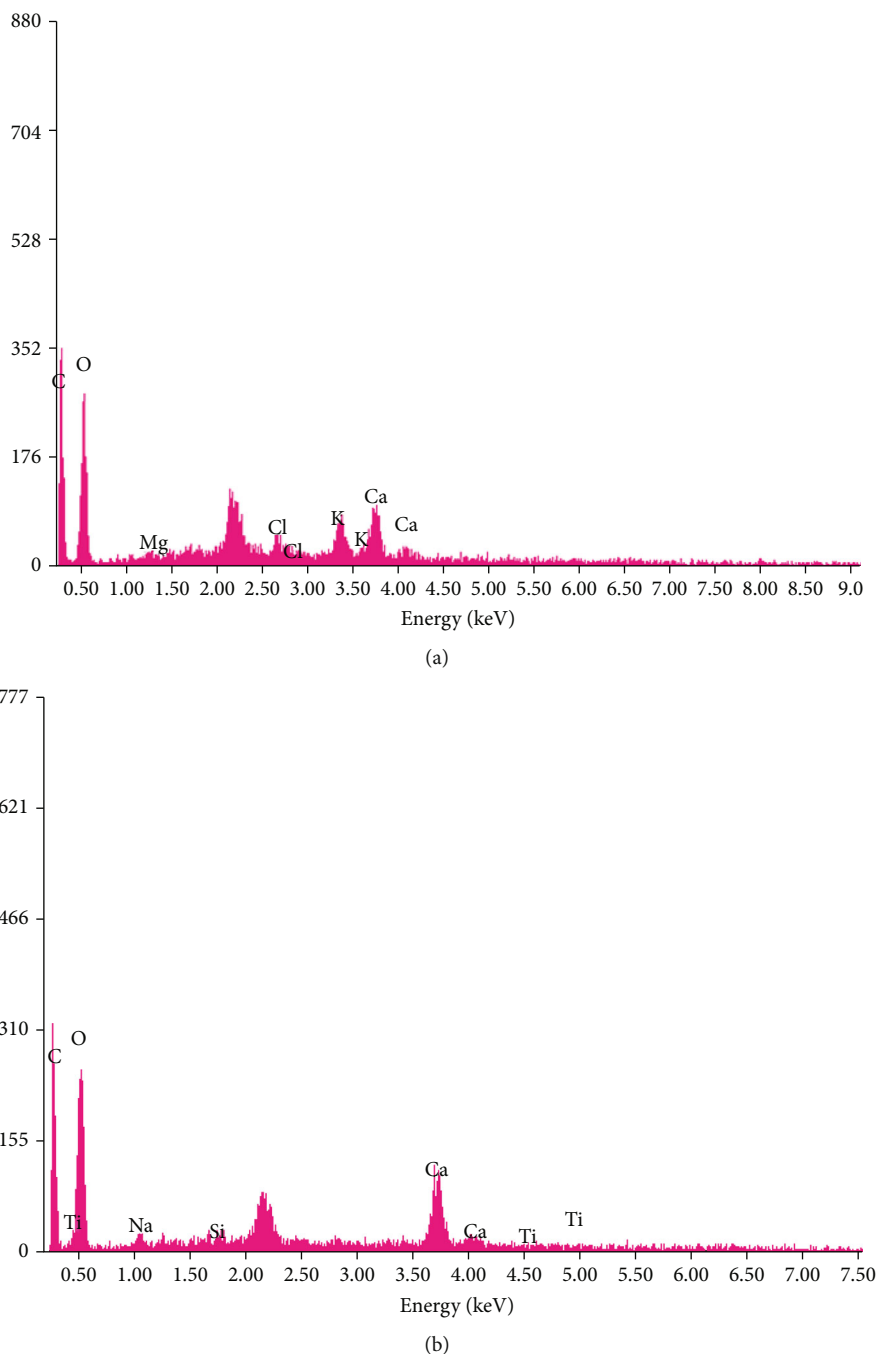


FIGURE 3: EDX patterns of (a) unmodified GP and (b) modified GP.

surging pH, the removal efficiency increased and reached peak at pH 6. Further increase in pH resulted in decrease of the removal efficiency. The increase in efficiency with respect to surging pH is due to reduction in H^+ ions concentration and competitive sorption for sites of active on MGP surface. The decrease in efficiency beyond pH 6 is due to surface of the garlic peel turning positive which could repel the adsorption of cationic dyes. This is successfully explained by the point zero charge of the adsorbent being at pH 5.7. Thus, pH 6 was fixed and set as optimum pH for the fixed-bed investigations of CV removal by MGP.

3.2. Fixed-Bed Column Investigations. The continuous investigations are carried out in a glass column packed with MGP by varying the key parameters of the column and the data obtained are represented in Table 1.

3.2.1. Flow Rate. The rate of flow in the continuous process greatly influences the rate of adsorption and it is considered a crucial parameter to be optimised prior to any scale-up process. Hence, the rate of flow of CV solution into the MGP packed column was investigated by changing the rate of flow and the data and BTC obtained are shown in

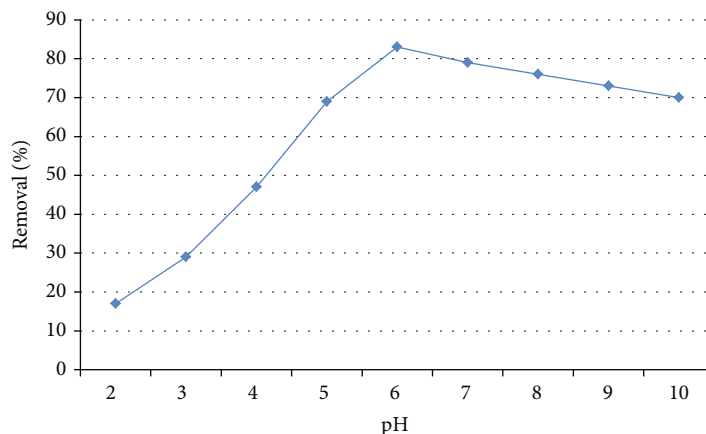


FIGURE 4: Optimization graph for pH for the removal of CV by MGP.

TABLE 1: Continuous column parameters for the removal of CV by MGP.

| C_0 (mg l ⁻¹) | Q (ml min ⁻¹) | H (cm) | D_{ad} (mg) | D_{total} (mg) | R (%) | EBCT (min) |
|-----------------------------|-----------------------------|----------|---------------|------------------|---------|------------|
| 100 | 3 | 1 | 18.08 | 45 | 45.1 | 1.57 |
| 100 | 5 | 1 | 14.4 | 55 | 26.3 | 1.17 |
| 100 | 7 | 1 | 7.2 | 52.5 | 13.7 | 0.15 |
| 100 | 3 | 2 | 51.4 | 105 | 48.9 | 2.38 |
| 100 | 3 | 3 | 99.9 | 169.5 | 58.9 | 3.56 |
| 200 | 3 | 3 | 59.6 | 225 | 26.4 | — |
| 300 | 3 | 3 | 41.4 | 216 | 19.1 | — |

Table 1 and Figure 5. It is seen that with increasing flow rate, the removal percentage and dye adsorption capacity plunged to lower values. The removal percentage decreased from 45.1% to 13.7% suggesting that lower flow rates are desirable. Similarly, the dye adsorption capacities decreased from 18.0 to 7.2 mg g⁻¹ suggesting that slower rate of flow increases the rate of adsorption. At low flow rates, the time of residence of CV molecules is high and hence, they have sufficed time to interact with the surface of the MGP to get adsorbed, while increasing the rate of flow decreases the residence time of CV molecules and thus the time of interaction with the surface decreases. Similar trend was reported for methyl green dye by mesoporous materials in continuous process [20].

3.2.2. Bed Height. Bed height is one another crucial parameter of fixed-bed analysis that can decide the economic feasibility of the continuous process. In view of the above, the bed height investigations were performed at different heights and the data and breakthrough curves obtained are summarised and represented in Table 1 and Figure 6. The data interestingly indicates that the percentage removal and loading capacity of MGP towards CV molecules surged with augmented bed heights. As seen from Table 1, the removal percentage increased from 45.1 to 58.9% and the loading capacity also improved significantly from 18.0 to 99.9 mg g⁻¹. The significant loading capacity observed is due to greater mass transfer zone due to increased bed depth of column.

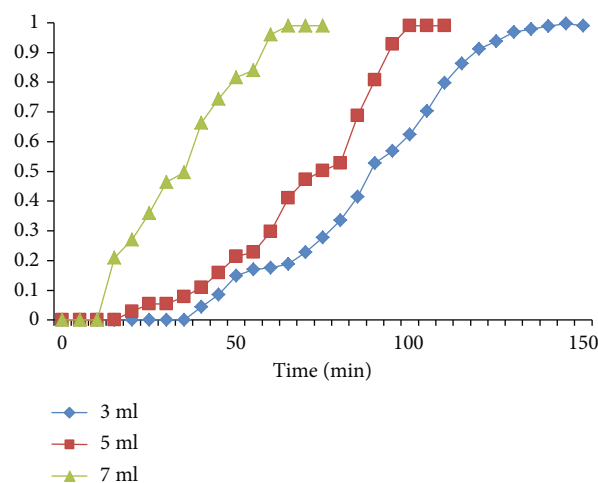


FIGURE 5: Breakthrough curves of variation of flow rate.

The column exhibits more adsorption sites at higher bed heights and thus greater is the adsorption capacity. Similar trend was observed and reported for the CV removal by activated carbon from bamboo leaves [21].

3.2.3. Initial Concentration. The initial concentration of CV solution finds a pivotal role in determining the efficiency and effectiveness of the fixed-bed columns. In order to know the influence of initial concentrations on the continuous

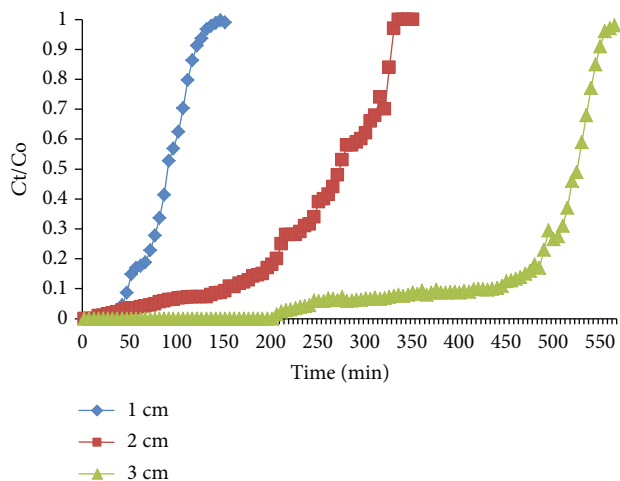


FIGURE 6: Breakthrough curves of variation of bed height.

process, experiments were run on varying the initial concentration of CV solution and the data and breakthrough curves are shown in Figure 7 and Table 1. It is noticed that with increasing initial concentrations, the breakthrough points started appearing early and in addition to that, the removal efficiency was significantly plunged to lower values. Following the trend, the loading capacity also went down from 99.9 mg g^{-1} to 41.4 mg g^{-1} . This is due to the competitive adsorption among the CV molecules at high concentrations and lack of surface active sites for adsorption. Similar trend was reported for CV removal by *Citrullus Lanatus* Rind in continuous studies [22].

3.3. Mathematical Models. Mathematical models play a crucial role in predicting the data and breakthrough curves obtained from continuous process and it is also handy in scaling up the bench scale process to industrial systems for real-time applications. In view of the above, various mathematical models and equations were developed for the purpose and in this study, most widely used models such as Adams-Bohart, Thomas, and Yoon-Nelson equations were adopted and applied for the data obtained.

3.3.1. Adams-Bohart Model. Continuous column data and the breakthrough curves are generally predicted with the Adams-Bohart model due to its ease of application and information obtained [23]. This model is helpful in predicting the initial breakthrough curves of the sorption system and suggests that the fraction of adsorbate coming is proportional to adsorption rate. The equation is given as

$$\ln \frac{C_t}{C_0} = k_{AB} C_0 t - k_{AB} N_0 \frac{z}{U_0}. \quad (5)$$

A graph of $(\ln C_0/C_t)$ vs t was plotted and the values of t were considered up to 0.5 of C_0/C_t from breakthrough curves and the constants such as K_{AB} and N_0 were determined from the slope and intercept of the linear plots obtained from equation (5) and summarised in Table 2. The K_{AB} values found to decrease with increasing rate of

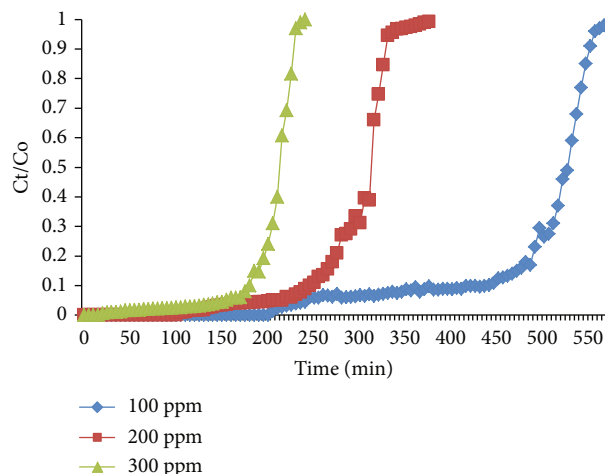


FIGURE 7: Breakthrough curves of variation of initial concentration.

flow and initial concentration and increases with augmenting bed heights. The correlation coefficients were also found to be moderately high indicating the applicability of the model for the initial part of the BCT's. The trend observed depicts that the external mass transfer is the dominating mechanism of the present system [7].

3.3.2. Thomas Model. The Thomas model is one of the realistic models that can describe the achievements of breakthrough curves perfectly [24]. This model can also estimate the loading capacity of the CV onto MGP from the linear plots. The formula/equation for the Thomas model is given as

$$\ln \left(\frac{C_0}{C_t} - 1 \right) = \frac{k_{Th} q_0 m}{Q} - k_{Th} C_0 t. \quad (6)$$

The linear plots of the Thomas model provided the constants from the slope and intercept and the values are summarised in Table 3. It is observed that the K_{Th} values increase with increasing flow rates and preliminary concentration and decrease with augmenting bed heights. In the case of q_0 , the trend was observed to be quite opposite to that of K_{Th} . The maximum loading capacity was estimated to be 97.4 mg g^{-1} which is very close to the experimental value 99.9 mg g^{-1} indicating the suitability of the model. The correlation coefficients support the better applicability of the model to the present CV removal onto MGP surface.

3.3.3. Yoon-Nelson Model. Another simplest model that can precisely explain the breakthrough curves is the Yoon-Nelson model which was originally developed to describe the gas phase molecule adsorption on to activated carbon [25]. The general expression is given as

$$\ln \left(\frac{C_t}{C_0 - C_t} \right) = k_{YN} t - \tau k_{YN}. \quad (7)$$

The constants of the Yoon-Nelson model derived from the linear plots are summarised in Table 4. It is observed that

TABLE 2: Parameters and constants of the Adams-Bohart model for the removal of CV by MGP.

| Parameter | | K_{AB} (l/mg min) | N_0 (mg/l) | R^2 |
|--|-----|----------------------|--------------|-------|
| Flow rate of solution (ml/min) | 3 | 1.4×10^{-5} | 11345 | 0.932 |
| | 5 | 1.1×10^{-5} | 13657 | 0.919 |
| | 7 | 1.0×10^{-5} | 15098 | 0.904 |
| Adsorbent depth (cm) | 1 | 1.4×10^{-5} | 11345 | 0.932 |
| | 2 | 1.7×10^{-5} | 10105 | 0.941 |
| | 3 | 2.3×10^{-5} | 9087 | 0.949 |
| Preliminary concentration (mg l^{-1}) | 100 | 2.3×10^{-5} | 9087 | 0.949 |
| | 200 | 2.0×10^{-5} | 11732 | 0.934 |
| | 300 | 1.8×10^{-5} | 12897 | 0.907 |

TABLE 3: Parameters and constants of the Thomas model for the removal of CV by MGP.

| Parameter | | K_{Th} (ml/min mg) | q_0 (mg/g) | R^2 |
|--|-----|----------------------|--------------|-------|
| Flow rate of solution (ml/min) | 3 | 2.1×10^{-3} | 45.7 | 0.989 |
| | 5 | 2.4×10^{-3} | 32.8 | 0.979 |
| | 7 | 2.6×10^{-3} | 29.7 | 0.971 |
| Adsorbent depth (cm) | 1 | 2.1×10^{-3} | 45.7 | 0.989 |
| | 2 | 1.9×10^{-3} | 69.9 | 0.991 |
| | 3 | 1.6×10^{-3} | 97.4 | 0.993 |
| Preliminary concentration (mg l^{-1}) | 100 | 1.6×10^{-3} | 97.4 | 0.993 |
| | 200 | 1.9×10^{-3} | 77.5 | 0.981 |
| | 300 | 2.6×10^{-4} | 58.8 | 0.975 |

TABLE 4: Parameters and constants of the Yoon-Nelson model for the removal of CV by MGP.

| Parameter | | K_{YN} (min^{-1}) | τ (min) | R^2 |
|--|-----|--------------------------------|--------------|-------|
| Flow rate of solution (ml/min) | 3 | 0.932 | 199.9 | 0.990 |
| | 5 | 0.918 | 173.0 | 0.985 |
| | 7 | 0.909 | 123.8 | 0.978 |
| Adsorbent depth (cm) | 1 | 0.932 | 199.9 | 0.990 |
| | 2 | 0.956 | 279.2 | 0.978 |
| | 3 | 0.977 | 323.8 | 0.963 |
| Preliminary concentration (mg l^{-1}) | 100 | 0.977 | 323.8 | 0.963 |
| | 200 | 0.963 | 239.7 | 0.954 |
| | 300 | 0.953 | 207.4 | 0.939 |

the K_{YN} and τ values decrease with increasing flow rate and preliminary concentrations and increase with increasing bed depths. The correlation coefficients obtained for the CV removal by MGP from Yoon-Nelson plots are high suggesting the applicability of this model as well to the present sorption system. The τ values found to be high for highest bed depths suggesting that the time for 50% exhaustion of column is high compared to other conditions.

3.4. Regeneration of MGP. Regeneration is an imperative step in adsorption process since it decides the economic via-

bility of the adsorbent and scale up for industrial process. Further disposal of CV-loaded MGP is not safe since it might contaminate the disposal sites. Keeping this in mind, investigations were performed to regenerate the MGP and recover the CV. To regenerate the MGP, various desorbing or regeneration agents were utilised such as 0.01 M HCl, 0.01 M NaOH, 0.01 M NaCl, and H_2O . It was found that regeneration of 0.01 M HCl exhibited highest regeneration efficiency compared to the other reagents selected in this study. The greater efficiency exhibited by the HCl is due to the competitive adsorption exhibited by the hydronium ions

on to the surface active sites. The regeneration efficiency was found to be in the following order $\text{HCl} > \text{NaOH} > \text{NaCl} > \text{H}_2\text{O}$. End of the investigation, concentrated CV solution was obtained and this can be reused in the dyeing industry with modifications in pH or recovered as solid by evaporation method.

4. Conclusion

The present investigation outlined the surface modification of garlic peel with NaOH and its applications in removal of crystal violet in continuous column mode. The analytical characterizations such as SEM and EDX confirmed the surface modification and porosity of the surface. The fixed-bed column investigations were performed at varying bed heights, flow rates, and initial concentrations and found that lower flow rates and initial concentrations with higher bed depths are desirable for optimum performance of the column. The mathematical methods were used for the column data and Thomas and Yoon-Nelson models explained the breakthrough patterns satisfactorily and can be used in scaling up the process for industrial applications. The regeneration efficiency showcased the reusability potential of the MGP. These results concluded that low-cost agro-waste such as garlic peel can be a prolific adsorbent for the remediation of crystal violet from wastewaters.

Data Availability

All the data required are available within the manuscript.

Conflicts of Interest

The authors declare no conflicts of interest.

References

- [1] <https://gahp.net/pollution-and-health-metrics/>.
- [2] S. Şahinkaya, "COD and color removal from synthetic textile wastewater by ultrasound assisted electro-Fenton oxidation process," *Journal of Industrial and Engineering Chemistry*, vol. 19, no. 2, pp. 601–605, 2013.
- [3] R. Lakshmipathy, M. K. Kesarla, A. R. Nimmala et al., "ZnS nanoparticles capped with watermelon rind extract and their potential application in dye degradation," *Research on Chemical Intermediates*, vol. 43, no. 3, pp. 1329–1339, 2017.
- [4] P. Ghosh, Swati, and I. S. Thakur, "Enhanced removal of COD and color from landfill leachate in a sequential bioreactor," *Bioresource Technology*, vol. 170, pp. 10–19, 2014.
- [5] R. Jayachandra, S. Rajasekhara Reddy, and R. Lakshmipathy, "D-Galactose based hydrophobic ionic liquid: a new adsorbent for the removal of Cd²⁺ ions from aqueous solution," *Environmental Progress & Sustainable Energy*, vol. 38, no. S1, pp. S139–S145, 2019.
- [6] P. Samiyammal, A. Kokila, L. Arul Pragasan et al., "Adsorption of brilliant green dye onto activated carbon prepared from cashew nut shell by KOH activation: studies on equilibrium isotherm," *Environmental Research*, vol. 212, p. 113497, 2022.
- [7] R. Lakshmipathy, G. L. Balaji, and I. L. R. Rico, "Removal of Pb²⁺ ions by ZSM-5/AC composite in a fixed-bed bench scale system," *Adsorption Science and Technology*, vol. 2021, article 2013259, pp. 1–8, 2021.
- [8] R. Biswa, S. N. Patra, A. K. Dalai, and V. Meda, "Taguchi-based process optimization for activation of agro-food waste biochar and performance test for dye adsorption," *Chemosphere*, vol. 285, p. 131531, 2021.
- [9] C. H. Nguyen, "Efficient removal of cationic dyes from water by a combined adsorption- photocatalysis process using platinum-doped titanate nanomaterials," *Journal of the Taiwan Institute of Chemical Engineers*, vol. 99, pp. 166–179, 2019.
- [10] C.-Y. Chen and W. J. Tseng, "Preparation of TiN-WN composite particles for selective adsorption of methylene blue dyes in water," *Advanced Powder Technology*, vol. 33, no. 2, p. 103423, 2022.
- [11] M. B. Surafel, V. P. Sundaramurthy, A. A. Temesgen, and C. Gomadurai, "A statistical modelling and optimization for Cr (VI) adsorption from aqueous media via Teff straw-based activated carbon: isotherm, kinetic and thermodynamic studies," *Adsorption Science and Technology*, vol. 2022, article 7998069, p. 16, 2022.
- [12] E. A. Kotenkova and N. V. Kupaeva, "Comparative antioxidant study of onion and garlic waste and bulbs," *IOP Conference Series: Earth and Environmental Science*, vol. 333, p. 012031, 2019.
- [13] B. H. Hameed and A. A. Ahmad, "Batch adsorption of methylene blue from aqueous solution by garlic peel, an agricultural waste biomass," *Journal of Hazardous Materials*, vol. 164, no. 2-3, pp. 870–875, 2009.
- [14] S. Liang, X. Guo, and Q. Tian, "Adsorption of Pb²⁺, Cu²⁺ and Ni²⁺ from aqueous solutions by novel garlic peel adsorbent," *Desalination and Water Treatment*, vol. 51, no. 37-39, pp. 7166–7171, 2013.
- [15] A. Asfaram, M. R. Fathi, S. Khodadoust, and M. Naraki, "Removal of Direct Red 12B by garlic peel as a cheap adsorbent: kinetics, thermodynamic and equilibrium isotherms study of removal," *Spectrochimica Acta Part A: Molecular and Biomolecular Spectroscopy*, vol. 127, pp. 415–421, 2014.
- [16] W. Liu, Y. Liu, Y. Tao, Y. Yu, H. Jiang, and H. Lian, "Comparative study of adsorption of Pb(II) on native garlic peel and mercerized garlic peel," *Environmental Science and Pollution Research*, vol. 21, no. 3, pp. 2054–2063, 2014.
- [17] Y. Zhao, W. Li, J. Liu et al., "Modification of garlic peel by nitric acid and its application as a novel adsorbent for solid-phase extraction of quinolone antibiotics," *Chemical Engineering Journal*, vol. 326, pp. 745–755, 2017.
- [18] S. S. Baral, N. Das, T. S. Ramulu, S. K. Sahoo, S. N. Das, and G. R. Chaudhury, "Removal of Cr(VI) by thermally activated weed *Salvinia cucullata* in a fixed- bed column," *Journal of Hazardous Materials*, vol. 161, no. 2-3, pp. 1427–1435, 2009.
- [19] A. A. Ahmad and B. H. Hameed, "Fixed-bed adsorption of reactive azo dye onto granular activated carbon prepared from waste," *Journal of Hazardous Materials*, vol. 175, no. 1-3, pp. 298–303, 2010.
- [20] S. M. Alardhi, T. M. Albayati, and J. M. Alrubaye, "Adsorption of the methyl green dye pollutant from aqueous solution using mesoporous materials MCM-41 in a fixed-bed column," *Helvion*, vol. 6, no. 1, p. e03253, 2020.
- [21] S. K. Ghosh, A. K. Hajra, and A. Bandyopadhyay, "Air agitated tapered bubble column adsorber for hazardous dye (crystal violet) removal onto activated (ZnCl₂) carbon prepared from

- bamboo leaves,” *Journal of Molecular Liquids*, vol. 240, pp. 313–321, 2017.
- [22] K. S. Bharathi and S. P. T. Ramesh, “Fixed-bed column studies on biosorption of crystal violet from aqueous solution by *Citrullus lanatus* rind and *Cyperus rotundus*,” *Applied Water Science*, vol. 3, no. 4, pp. 673–687, 2013.
- [23] G. Bohart and E. Q. Adams, “Some aspects of the behavior of charcoal with respect to CHLORINE.1,” *Journal of American Chemical Society*, vol. 42, no. 3, pp. 523–544, 1920.
- [24] H. C. Thomas, “Heterogeneous ion exchange in a flowing system,” *Journal of American Chemical Society*, vol. 66, no. 10, pp. 1664–1666, 1944.
- [25] Y. H. Yoon and J. H. Nelson, “Application of gas adsorption kinetics I. A theoretical model for respirator cartridge service life,” *American Industrial Hygiene Association Journal*, vol. 45, no. 8, pp. 509–516, 1984.